

Journal of Organometallic Chemistry, 224 (1981) 237–245
Elsevier Sequoia S.A., Lausanne — Printed in The Netherlands

HEXAORGANO-SUBSTITUTED TRIATOMICS R_3XYZR_3 : THE CONFIGURATIONS OF ORGANOMETALLIC SULPHIDES $(R_3M)_2S$ AND THE CRYSTAL AND MOLECULAR STRUCTURE OF THIO-BIS[TRIPHENYLTIN(IV)]

CHRISTOPHER GLIDEWELL * and DAVID C. LILES

Chemistry Department, University of St. Andrews, St. Andrews, Fife KY16 9ST (Great Britain)

(Received August 26th, 1981)

Summary

Crystals of thio-bis[triphenyltin(IV)], $S(Ph_3Sn)_2$, are orthorhombic, space-group $P2_12_12_1$, with $a = 18.469(5)$, $b = 17.648(5)$, $c = 9.848(6)$ Å and $Z = 4$. The SnS distances are 2.405(9) and 2.417(7) Å and SnSSn angle is $107.3(2)^\circ$: there are no anomalous features in the structure analogous to those in $O(Ph_3Sn)_2$. MNDO calculations for a series of organometallic sulphides $(Me_3M)_2S^{+n}$ ($M = Be, B, C, N, Si, P$) indicate that the inversion barrier to linearity increases monotonically, and the skeletal bending force constant at linearity decreases correspondingly as the group Me_3M becomes more electro-negative.

Introduction

We have recently reported the occurrence of very wide MOM skeletal angles in $(Ph_3M)_2O$ and $[(PhCH_2)_3M]_2O$ [1–6]: in each of the benzyl derivatives, and in $(Ph_3Si)_2O$, the molecules lie across crystallographic centres of inversion, so that the MOM fragments are strictly linear. The linearity at oxygen was accounted for in terms of a model based on the second-order Jahn-Teller effect [7,8], and this model has been supported by an extensive series of calculations in the MINDO and MNDO approximations [9–12]. As part of this study, we are determining the structures of selected sulphur analogues $(R_3M)_2S$, and here we report the structure of $(Ph_3Sn)_2S$, together with the results of MNDO calculations of equilibrium structures, inversion barriers, and skeletal bending force constants for a wide range of simple sulphides. The structures of the analogous $(Ph_3Ge)_2S$ and $Ph_3SnSPbPh_3$ have been reported previously [13,14] as has that of the selenide $(Ph_3Sn)_2Se$ [15].

* To receive correspondence.

Experimental

Thio-bis[triphenyltin(IV)], $S(\text{Ph}_3\text{Sn})_2$, was prepared by the reaction between Ph_3SnCl and Na_2S in ethanol. Crystals suitable for X-ray investigation were grown from 60–80 petrol solution.

Data collection

Data were collected using a Stoe Stadi-2 two circle automatic diffractometer with graphite monochromatised Mo-K_α radiation for a crystal of dimensions $0.1 \times 0.1 \times 0.5$ mm mounted about c . The intensities of 2234 reflections in the octant $+h, +k, +l$ with $2^\circ \leq \theta \leq 30^\circ$, $l = 0-12$ ($0 \leq \mu \leq 25.658^\circ$) were measured using the $\omega-2\theta$ scan mode. Standard reflections were measured every 50 reflections and showed only small random deviations from their mean values. Lorentz and polarisation corrections were applied to the data, but no corrections for absorption was made.

Crystal data

Thio-bis[triphenyltin(IV)], $\text{C}_{36}\text{H}_{30}\text{SSn}_2$, $M_r = 732.08$. Orthorhombic, space group $P2_12_12_1$ (D_2^4 , No. 19) $a = 18.469(5)$, $b = 17.648(5)$, $c = 9.848(6)$ Å; $U = 3209.87$ Å³; $Z = 4$; $D_c = 1.515$ Kg dm⁻³; $F(000) = 1488$. Mo-K_α radiation, $\lambda = 0.71069$ Å, $\mu(\text{Mo-K}_\alpha) = 15.08$ cm⁻¹.

Structure solution and refinement

These were carried out using SHELX-76 [16] for 2157 reflections having $I_0 > 2\sigma(I_0)$. The structure was solved using Patterson and weighted difference syntheses and was refined by full-matrix least-squares with individual isotropic temperature parameters for all non-hydrogen atoms to yield a conventional R index [$= \Sigma \Delta / \Sigma F_0$, ($\Delta = |F_0 - F_c|$)] of 0.1124 and a generalised index R_G [$= (\Sigma w \Delta^2 / \Sigma w F_0^2)^{1/2}$] of 0.1412. With the least-squares matrix blocked such that the parameters for S refined in every cycle and the parameters for the two Ph_3Sn fragments refined in alternate cycles, and anisotropic temperature parameters for all non-hydrogen atoms, the refinement converged to give $R = 0.0834$ and $R_G = 0.0939$. The introduction of hydrogen atoms in calculated positions ($\text{C-H} = 1.08$ Å), with common isotropic temperature parameters for the hydrogens in each half of the molecule, reduced R to 0.0793 and R_G to 0.0870. A similar refinement of the alternative enantiomorph yielded $R = 0.0798$ and $R_G = 0.0874$. In the final cycles of refinement 354 parameters were varied comprising of 117 positional parameters, 234 anisotropic temperature parameters, 2 isotropic temperature parameters, and 1 overall scale factor. A final difference synthesis showed no significant residual features. The reductions in R_G at all stages of the refinement were significant at the 99.5% level [17]. Complex neutral-atom scattering factors [18] were employed for all atoms. The results of the final least-squares cycles are given in Tables 1 and 2. These, together with the full-covariance matrix were used to calculate the bond lengths and angles which are given with e.s.d.'s in Tables 3 and 4. Least-squares planes were calculated for each phenyl ring: these are given in Table 5. Figure 1 is a perspective view of the molecule showing the atom numbering scheme. Figure 2 shows the unit cell contents.

TABLE 1

TOM FRACTIONAL COORDINATES ($\times 10^4$) AND THE EQUIVALENT ISOTROPIC TEMPERATURE PARAMETERS (U_{iso})^a ($\text{\AA}^2, \times 10^{-3}$)

tom	x	y	z	U_{iso}
1(1)	5920(1)	4707(1)	-773(2)	40(1)
1(2)	4499(1)	3683(1)	1481(2)	39(1)
	5042(4)	4899(3)	998(9)	49(4)
(111)	6377(13)	3529(11)	-802(29)	23(13)
(112)	6078(13)	3020(13)	-1629(26)	32(14)
(113)	6370(18)	2317(15)	-1639(32)	42(16)
(114)	6973(18)	2108(17)	-870(52)	64(27)
(115)	7246(14)	2674(17)	8(42)	54(21)
(116)	6947(17)	3441(15)	-25(36)	55(20)
(121)	5412(15)	4935(12)	-2656(28)	36(15)
(122)	4750(16)	5257(19)	-2893(42)	60(22)
(123)	4473(21)	5415(18)	-4084(63)	76(32)
(124)	4827(19)	5323(23)	-5273(47)	79(27)
(125)	5530(23)	5031(18)	-5125(34)	68(23)
(126)	5817(20)	4812(19)	-3826(30)	62(23)
(131)	6779(18)	5571(17)	-357(40)	55(22)
(132)	6774(15)	5909(14)	904(34)	33(17)
(133)	7321(21)	6432(20)	1138(41)	74(24)
(134)	7810(22)	6560(20)	175(56)	76(31)
(135)	7774(23)	6117(33)	-959(43)	93(37)
(136)	7261(17)	5610(20)	-1248(46)	65(27)
(211)	3545(15)	4068(15)	2641(31)	37(17)
(212)	3179(12)	3577(18)	3403(36)	45(18)
(213)	2583(17)	3779(22)	4103(39)	64(23)
(214)	2357(18)	4490(23)	4019(36)	59(25)
(215)	2691(17)	4991(19)	3190(43)	69(25)
(216)	3320(16)	4742(18)	2487(46)	64(25)
(221)	5151(15)	2917(17)	2788(32)	33(19)
(222)	5012(17)	2874(21)	4054(45)	70(25)
(223)	5329(19)	2305(22)	4878(39)	71(26)
(224)	5853(24)	1846(17)	4246(55)	49(30)
(225)	5935(20)	1875(16)	2922(51)	48(27)
(226)	5627(15)	2472(16)	2054(42)	65(22)
(231)	4218(12)	3147(14)	-392(30)	28(15)
(232)	3955(12)	3582(17)	-1405(35)	39(18)
(233)	3742(15)	3241(18)	-2707(34)	53(20)
(234)	3774(20)	2440(22)	-2809(39)	60(28)
(235)	4020(18)	2031(16)	-1731(33)	54(19)
(236)	4239(14)	2332(14)	-530(31)	48(17)

U_{iso} is defined as the geometric mean of the diagonal components of the diagonalised matrix of U_{ij} .

Molecular energies

Calculations of molecular structures and energies were made using MNDO 19]: for species $(\text{H}_3\text{M})_2\text{S}^{+n}$, complete optimisation of all geometrical variables was undertaken at a series of values of the angle $\angle\text{MSM}$, and hence a relaxed potential energy curve was derived: from this the inversion barrier, and the skeletal bending force-constant were derived. All points having non-linear skeletons optimised to exact C_{2v} symmetry, with four close and two distant hydrogens: equilibrium values of $d(\text{M}-\text{S})$, $\angle(\text{MSM})$ and ΔH_f^θ are recorded in Table 6, together with inversion barriers at linearity and skeletal bending force

TABLE 2

ANISOTROPIC TEMPERATURE PARAMETERS (\AA^2 , $\times 10^{-3}$)

	U_{11}	U_{22}	U_{33}	U_{23}	U_{13}	U_{12}
Sn(1)	39(1)	32(1)	52(1)	-1(1)	-2(1)	-6(1)
Sn(2)	33(1)	34(1)	54(1)	1(1)	2(1)	2(1)
S	65(5)	30(3)	73(6)	-7(4)	25(4)	-7(3)
C(111)	56(15)	25(11)	40(13)	-2(13)	-13(14)	32(11)
C(112)	55(16)	44(13)	31(14)	25(13)	-17(13)	-11(13)
C(113)	94(23)	44(15)	48(19)	35(15)	-15(18)	0(16)
C(114)	70(21)	45(18)	163(42)	-53(26)	42(28)	3(17)
C(115)	24(13)	53(18)	133(32)	5(21)	11(18)	9(13)
C(116)	61(19)	40(16)	93(25)	-27(17)	-6(19)	13(15)
C(121)	50(17)	19(11)	54(17)	-1(11)	-17(15)	-3(12)
C(122)	49(18)	56(19)	106(29)	23(22)	-29(19)	9(17)
C(123)	83(26)	57(20)	187(51)	28(30)	2(37)	45(20)
C(124)	56(21)	84(26)	111(35)	-21(27)	-25(22)	7(21)
C(125)	103(28)	78(24)	51(19)	-3(17)	-34(21)	4(22)
C(126)	105(27)	95(24)	47(19)	27(18)	-5(18)	53(23)
C(131)	56(19)	50(16)	110(32)	-6(18)	-51(21)	-8(16)
C(132)	60(17)	44(15)	69(21)	-28(16)	-16(17)	-29(14)
C(133)	105(29)	69(24)	77(29)	1(20)	-44(24)	13(23)
C(134)	82(28)	56(22)	139(44)	28(26)	-46(30)	1(20)
C(135)	90(29)	234(59)	46(24)	11(33)	-24(23)	17(37)
C(136)	47(18)	92(25)	125(39)	-19(25)	-39(24)	-23(19)
C(211)	54(17)	47(15)	64(20)	29(15)	-43(16)	-14(14)
C(212)	19(11)	75(20)	88(23)	12(21)	17(16)	-9(13)
C(213)	68(21)	85(24)	81(25)	41(24)	4(20)	-30(21)
C(214)	64(20)	119(32)	57(23)	0(22)	37(18)	-35(23)
C(215)	71(23)	62(19)	114(33)	17(21)	19(24)	36(18)
C(216)	48(17)	54(18)	175(41)	37(26)	49(23)	17(16)
C(221)	39(16)	67(20)	55(20)	-15(17)	31(15)	17(14)
C(222)	42(18)	85(25)	110(32)	-24(26)	17(22)	5(18)
C(223)	68(25)	100(29)	68(23)	32(22)	-7(19)	22(22)
C(224)	113(32)	44(18)	151(40)	47(25)	-113(34)	-26(21)
C(225)	76(23)	35(16)	158(42)	-11(21)	-66(28)	35(17)
C(226)	49(19)	48(17)	122(31)	-20(19)	5(20)	-10(15)
C(231)	28(13)	43(14)	74(21)	-18(14)	-25(13)	-15(11)
C(232)	29(12)	67(18)	89(23)	48(20)	3(16)	-22(14)
C(233)	47(17)	73(21)	59(21)	-20(17)	-17(16)	-12(15)
C(234)	96(29)	105(30)	73(25)	-60(24)	22(22)	-62(25)
C(235)	74(20)	47(16)	59(21)	-19(16)	-20(19)	-5(16)
C(236)	58(18)	33(13)	61(20)	5(13)	5(15)	-5(12)

The isotropic temperature parameters for the hydrogens in each half of the molecule refined to 0.08(3) and 0.10(3) \AA^2 .

TABLE 3

BOND DISTANCES (\AA)

Sn(1) ··· Sn(2)	3.883(3)	Sn(1)—S	2.405(9)	Sn(2)—S	2.417(7)
Sn(1)—C(111)	2.24(2)	Sn(1)—C(121)	2.12(3)	Sn(1)—C(131)	2.24(3)
Sn(2)—C(211)	2.21(3)	Sn(2)—C(221)	2.22(3)	Sn(2)—C(231)	2.14(3)

Within the phenyl rings C(*ijk*)—C(*ijl*)

<i>k</i> — <i>l</i>	<i>ij</i>					
	11	12	13	21	22	23
1—2	1.33(3)	1.37(4)	1.38(5)	1.33(4)	1.28(5)	1.35(4)
2—3	1.35(4)	1.31(7)	1.39(5)	1.35(4)	1.42(5)	1.47(5)
3—4	1.40(5)	1.35(7)	1.33(6)	1.33(5)	1.41(6)	1.42(5)
4—5	1.41(5)	1.41(5)	1.37(7)	1.35(5)	1.31(7)	1.36(5)
5—6	1.46(4)	1.44(5)	1.33(6)	1.42(5)	1.47(5)	1.36(4)
6—1	1.31(4)	1.39(4)	1.25(5)	1.27(4)	1.38(4)	1.45(3)

TABLE 4
OND ANGLES (°)

n(1)—S—Sn(2)	107.3(3)	S—Sn(2)—C(211)	99.2(7)
—Sn(1)—C(111)	113.2(7)	S—Sn(2)—C(221)	115.5(8)
—Sn(1)—C(121)	108.0(8)	S—Sn(2)—C(231)	108.9(7)
—Sn(1)—C(131)	104.4(10)	C(211)—Sn(2)—C(221)	108.7(11)
(111)—Sn(1)—C(121)	109.4(9)	C(211)—Sn(2)—C(231)	112.9(10)
(111)—Sn(1)—C(131)	115.5(10)	C(221)—Sn(2)—C(231)	111.3(10)
(121)—Sn(1)—C(131)	110.2(12)		

within the phenyl rings C(*ijk*)—C(*ijl*)—C(*ijm*)/Sn(*i*)

<i>ij</i>	<i>ij</i>					
	11	12	13	21	22	23
—l—m/Sn(<i>i</i>)						
—2—3	117(3)	126(4)	116(3)	122(3)	121(3)	121(3)
—3—4	124(3)	124(4)	119(4)	118(3)	116(4)	117(3)
—4—5	115(3)	114(4)	117(4)	121(3)	120(4)	119(3)
—5—6	120(3)	122(4)	126(4)	118(3)	124(3)	125(3)
—6—1	115(3)	120(3)	113(4)	120(3)	111(4)	125(3)
—1—2	128(2)	114(3)	128(3)	121(3)	127(3)	120(3)
—1—Sn(<i>i</i>)	119(2)	129(2)	117(2)	120(2)	120(2)	118(2)
—1—Sn(<i>i</i>)	114(2)	117(2)	114(3)	119(2)	113(2)	121(2)

TABLE 5

EAST-SQUARES PLANES THROUGH THE PHENYL CARBON ATOMS C(*ijk*), DISTANCES OF POINTS FROM THE PLANES AND DIHEDRAL ANGLES BETWEEN THE PLANES

The planes are defined in orthogonal Ångström coordinates by the equation $Ax + By + Cz + D = 0$

<i>ij</i>	<i>ij</i>					
11	12	13	21	22	23	
0.615(3)	0.387(2)	−0.553(3)	−0.568(3)	−0.750(2)	0.933(1)	
0.280(2)	−0.918(2)	0.724(5)	−0.270(2)	−0.631(6)	0.745(2)	
−0.738(15)	−0.860(5)	−0.412(4)	−0.777(7)	−0.200(12)	−0.353(2)	
−9.56(3)	11.65(2)	−0.29(5)	7.66(3)	10.93(4)	−7.79(2)	

Distances of atoms from the planes (Å × 10^{−2})

<i>ij</i> 1)	−1(4)	0(3)	5(6)	−2(4)	0(5)	2(3)
<i>ij</i> 2)	0(3)	−2(4)	−2(5)	2(4)	−1(6)	−3(3)
<i>ij</i> 3)	0(4)	2(4)	−1(6)	1(4)	3(6)	2(4)
<i>ij</i> 4)	2(5)	2(5)	5(6)	−3(4)	−6(6)	0(4)
<i>ij</i> 5)	−3(4)	−3(4)	−3(7)	2(4)	5(6)	−1(4)
<i>ij</i> 6)	3(4)	1(4)	−3(6)	1(4)	−2(5)	−1(3)
(<i>i</i>)	2(3)	−15(2)	−1(5)	5(3)	31(4)	−8(2)

Dihedral angles between planes C(*ijk*) and C(*lmk*) (*k* = 1—6) (°)

<i>lm</i>	<i>ij</i>	<i>lm</i>	<i>ij</i>	<i>lm</i>	<i>ij</i>	<i>lm</i>
12	−64.6(3)	11 13	80.6(4)	11 21	81.4(3)	11 22
23	31.2(2)	12 13	−65.5(4)	12 21	57.7(3)	12 22
23	−66.5(2)	13 21	64.0(8)	13 22	87.7(6)	13 23
22	41.3(9)	21 23	−74.0(8)	22 23	−47.5(5)	

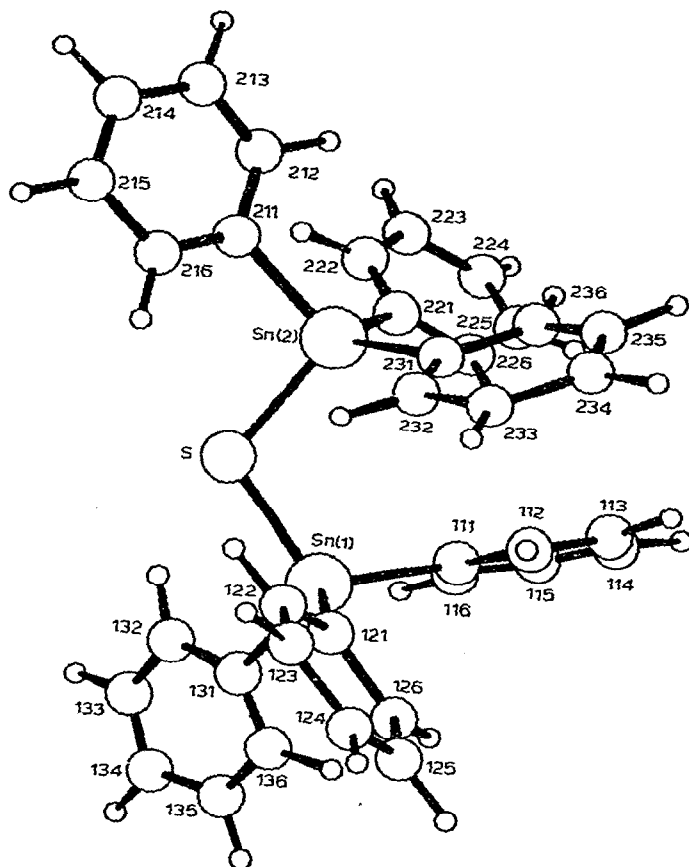


Fig. 1. A perspective view of the molecule showing the atom numbering scheme. Numbers without a preceding letter refer to carbon atoms.

constants at linearity. For the permethyl species $(\text{Me}_3\text{M})_2\text{S}^{+n}$ force constants were not calculated directly, but rather two optimisations were performed for each, one fully optimised and one with the angle $\angle\text{MSM}$ constrained to 180° : equilibrium properties and inversion barriers are given in Table 7. For both

TABLE 6

EQUILIBRIUM PROPERTIES, INVERSION BARRIERS ΔE , AND FORCE CONSTANTS AT LINEARITY FOR $(\text{H}_3\text{M})_2\text{S}^{+n}$

	$d(\text{M}-\text{S})$ (Å)	$\angle(\text{MSM})$ (°)	ΔH_f^\ominus (kJ mol ⁻¹)	ΔE (kJ mol ⁻¹)	f (Nm ⁻¹)
$(\text{H}_3\text{Be})_2\text{S}^{-4}$	2.228	141.4	+1784.7	+9.22	-119.3
$(\text{H}_3\text{B})_2\text{S}^{-2}$	1.810	112.7	-57.5	+138.8	-127.4
$(\text{H}_3\text{C})_2\text{S}$	1.733	107.6	-72.7	+217.5	-231.5
$(\text{H}_3\text{N})_2\text{S}^{+2}$	1.709	111.0	+2038.5	+311.6	-545.6
$(\text{H}_3\text{Si})_2\text{S}$	2.061	108.9	-70.3	+60.3	-35.1
$(\text{H}_3\text{P})_2\text{S}^{+2}$	1.982	114.3	+2098.2	+221.6	-372.2

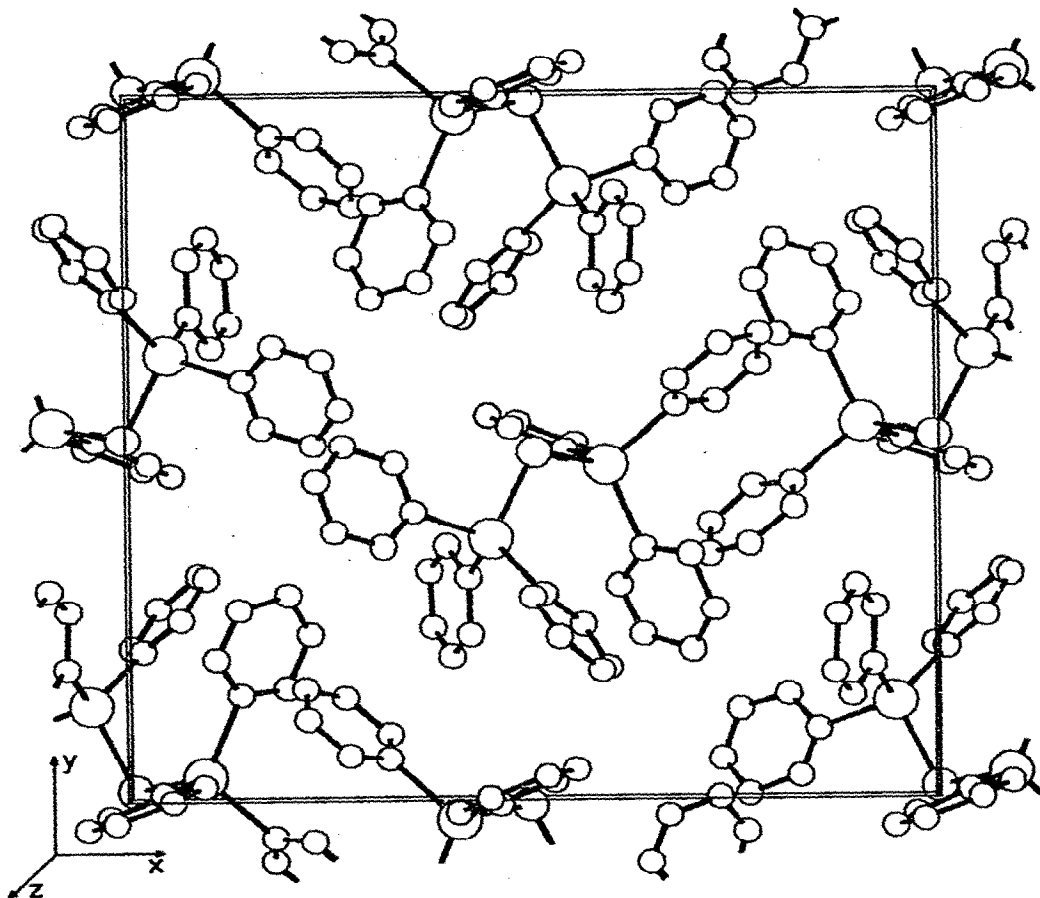


Fig. 2. The unit cell contents viewed from the z direction.

$(\text{H}_3\text{S})_2\text{S}^{+4}$ and $(\text{Me}_3\text{S})_2\text{S}^{+4}$ the attempted optimisations were unsatisfactory, converging in the perhydro case to a minimum with very long S—S bonds, while for the permethyl ion, dissociation occurred with loss of a methyl group from each terminal sulphur.

TABLE 7
EQUILIBRIUM PROPERTIES, AND INVERSION BARRIERS ΔE , FOR $(\text{Me}_3\text{M})_2\text{S}^{+n}$

	$d(\text{M}-\text{S})$ (Å)	$d(\text{M}-\text{C})$ (Å)	$\angle(\text{MSM})$ (°)	ΔH_f^\ominus (kJ mol ⁻¹)	ΔE (kJ mol ⁻¹)
$(\text{Me}_3\text{Be})_2\text{S}^{-4}$	2.215	1.835	141.2	+1033.9	+11.3
$(\text{Me}_3\text{B})_2\text{S}^{-2}$	1.857	1.611	123.8	-356.7	+117.2
$(\text{Me}_3\text{C})_2\text{S}$	1.777	1.549	121.9	-98.5	+176.6
$(\text{Me}_3\text{N})_2\text{S}^{+2}$	1.731	1.551	122.7	+2040.5	+295.4
$(\text{Me}_3\text{Si})_2\text{S}$	2.079	1.853	123.2	-703.3	+43.8
$(\text{Me}_3\text{P})_2\text{S}^{+2}$	1.992	1.824	121.6	+1436.4	+171.7

Results and discussion

The structure comprises isolated molecules with no close intermolecular contacts. The Sn—S distances (mean 2.411(8) Å) are comparable to the distance 2.44(2) Å found in $\text{Ph}_3\text{SnSPbPh}_3$ [14] and to the values found in a number of triphenyltinthiophenolates (range 2.413–2.459 Å, mean 2.433(20) Å) [20,21]. The Sn—C distances (mean 2.19(5) Å) and the S—Sn—C and C—Sn—C angles (mean 108.2° and 111.3° respectively) are all typical values for triphenyltin compounds [3,14,15,20,21]. The Sn—S—Sn angle of 107.3(3)° is identical within experimental error to the Sn—S—Pb angle of 107.2(10)° in $\text{Ph}_3\text{SnSPbPh}_3$ [14], and compares with the Ge—S—Ge angle of 111.0(3)° (mean value from 2 crystal modifications) in $(\text{Ph}_3\text{Ge})_2\text{S}$ [13], the Sn—Se—Sn angle of 104.3(10)° (mean) in $(\text{Ph}_3\text{Sn})_2\text{Se}$ [15] and the Sn—S—C angles (range 98.2–105.0°, mean 101(3)°) in triphenyltinthiophenolates [20,21]. The Sn—S bond lengths and the Sn—S—Sn bond angle indicate there is no significant Sn—S π bonding. The Sn—O—Sn angle in the oxygen homologue of 137.3(1) [3] is significantly larger but this can be ascribed to a “hard atom” contact between the two Sn atoms [3]: the Sn...Sn distances in the O, S and Se homologues are 3.641, 3.883(3) and 3.990(4) Å respectively. The conformation of the molecule is almost staggered. The dihedral angles C(1*i*1)—Sn(1)...Sn(2)—C(2*i*1) for $i = 1$ and 3 are 175.9(11) and $-179.5(13)^\circ$ respectively. For $i = 2$ the dihedral angle is $-148.6(10)^\circ$, this apparent discrepancy may be explained in terms of the tilt of the two Ph_3SnS fragments with respect to the Sn...Sn direction due to the Sn—S—Sn angle of 107.3(3). The projection of the Sn—S bonds onto a plane perpendicular to the Sn...Sn direction approximately bisects the external C(121)—Sn(1)...Sn(2)—C(221) dihedral angle.

The data of Table 6 show that for $(\text{H}_3\text{M})_2\text{S}^{+n}$ the skeletal angle $\angle\text{MSM}$ is extremely large for $\text{M} = \text{Be}$, although not so for other M: as expected the M—S distance decreases in the order $\text{Be} > \text{B} > \text{C} > \text{N}$ and $\text{S} > \text{P}$. It is striking that as M varies from Be to N, i.e. as H_3M becomes more electronegative, the force constant for skeletal bending computed at the linear configuration becomes steadily more negative, indicative of a steadily greater tendency of the linear configuration to bend. This is in accordance with the hypothesis put forward earlier [7,8], and with the behaviour of other similar series [11,12]. At the same time as the force constant is varying monotonically to more negative values as H_3M becomes more electronegative, so also the barrier to inversion moves steadily to more positive values: this correlation is one we have noted previously [12], and the partial series of second row $\text{M} = \text{Si}, \text{P}$ shows the same trend.

Accordingly we have assumed that such variations as may be found to occur in the inversion barriers in $(\text{Me}_3\text{M})_2\text{S}^{+n}$ will be a reflection of the variations which occur in the skeletal bending force constant within this series. Subject to this assumption we deduce from the variation in ΔE in $(\text{Me}_3\text{M})_2\text{S}^{+n}$ (Table 7) that again the force constant, at linearity, for skeletal bending is always negative, and moves smoothly to more negative values as M varies $\text{Be} > \text{B} > \text{C} > \text{N}$ and $\text{Si} > \text{P}$, just as for the series $(\text{H}_3\text{M})_2\text{S}^{+n}$. We have previously shown [7,8,11,12] that the second-order Jahn-Teller effect provides an excellent rationalisation for the geometrical properties of species $(\text{R}_p\text{M})_2\text{X}^{+n}$ in circum-

ances when X is an element of the first Periodic row. The present work shows that the same model can be applied to species in which X is an element of the second row, and the similar conclusion must follow; namely that when the ligand R_pM is of low electronegativity relative to the central atom X, the angular geometry at X will be anomalous in the context of the VSEPR and the stereochemical influence of the non-bonding electrons formally locally on X will be weak: this is well exemplified in the cases $(H_3Be)_2S^{-4}$ and $(Me_3Be)_2S^{-4}$ where the angles at sulphur are calculated to be 141.4° and 141.2° , respectively.

No examples have yet been described experimentally in which the interbond angles at sulphur approach those found in certain μ -oxo compounds and related species [1-6]: this is simply a consequence of the lower electronegativity of sulphur compared with oxygen. To attain a difference in electronegativity in a compound $(R_pM)_2S^{+n}$ between R_pM and S which is sufficient to eliminate most or all of the stereochemical influence of the lone pairs on sulphur, the ligand R_pM must be of much lower electronegativity than would be required in the analogous $(R_pM)_2O^{+n}$ species: it seems likely that only anionic ligands will in practice be of sufficiently low electronegativity for the manifestation of stereochemically inactive lone pairs to occur.

References

1. C. Glidewell and D.C. Liles, *Acta Cryst.*, B, 34 (1978) 119.
2. C. Glidewell and D.C. Liles, *Acta Cryst.*, B, 34 (1978) 124.
3. C. Glidewell and D.C. Liles, *Acta Cryst.*, B, 34 (1978) 1693.
4. C. Glidewell and D.C. Liles, *Acta Cryst.*, B, 35 (1979) 1689.
5. C. Glidewell and D.C. Liles, *J. Organometal. Chem.*, 174 (1979) 275.
6. C. Glidewell and D.C. Liles, *J. Organometal. Chem.*, 212 (1981) 291.
7. C. Glidewell, *Inorg. Chim. Acta*, 29 (1978) L283.
8. C. Glidewell, *J. Organometal. Chem.*, 159 (1978) 23.
9. C. Glidewell, *J. Mol. Structure*, 65 (1980) 231.
10. C. Glidewell, *J. Mol. Structure*, 67 (1980) 121.
11. A.F. Cuthbertson and C. Glidewell, *J. Mol. Structure*, in press.
12. A.F. Cuthbertson, C. Glidewell, and D.C. Liles, *J. Mol. Structure*, submitted.
13. B. Krebs and H.-J. Korte, *J. Organometal. Chem.*, 179 (1979) 13.
14. H. Schumann and P. Reich, *Z. Anorg. Allgem. Chem.*, 377 (1970) 63.
15. B. Krebs and H.-J. Jacobson, *J. Organometal. Chem.*, 178 (1979) 301.
16. G.M. Sheldrick, SHELX-76 program system, Cambridge, (1976).
17. W.C. Hamilton, *Acta Cryst.*, 18 (1965) 502.
18. D.T. Cromer and J.B. Mann, *Acta Cryst.*, A, 24 (1968) 321.
19. M.J.S. Dewar and W. Thiel, *J. Amer. Chem. Soc.*, 99 (1977) 489; W. Thiel, *QCPE*, XI (1979) 353.
20. P.L. Clarke, M.E. Cradwick, and J.L. Wardell, *J. Organometal. Chem.*, 63 (1973) 279.
21. N.G. Bokii, Yu.T. Struchkov, D.N. Kravtsov, and E.M. Rokhlina, *Zh. Strukt. Khim.*, 14 (1973) 291: 15 (1974) 497.